References

[1] Hedgepeth, J. M., "Flutter of Rectangular Simply Supported Panels at High Supersonic Speeds," *Journal of Aeronautical Sciences*, Vol. 24, 1957, pp. 563–573, 586.

[2] Eisley, J. G. and Luessen, G., "The Flutter of Thin Plates Under Combined Shear and Normal Edge Forces Including the Effects of Varying Sweepback," *AIAA Journal*, Vol. 1, No. 3, March 1963, p. 620.

[3] Durvasula, S., "Flutter of Simply Supported Parallelogrammic Flat Panels in Supersonic Flow," *AIAA Journal*, Vol. 5, No. 9, Sept. 1967, pp. 1668–1673.

[4] Kariappa and Somashekar, B. R., "Application of Matrix Displacement Methods in the Study of Panel Flutter," *AIAA Journal*, Vol. 7, No. 1, Jan. 1969, pp. 50–53.

[5] Argyris, J. H., "Matrix Displacement Analysis of Plates and Shells," *Ingenieur-Archiv*, XXXV Band 1966.

[6] Schaeffer, H. G. and Heard, H. L., "Flutter of a Flat Panel Subjected to a Nonlinear Temperature Distribution," *AIAA Journal*, Vol. 3, No. 10, Oct. 1965, pp. 1918–1923.

[7] Lemley, C. E., "Design Criteria for the Prediction and Prevention of Panel Flutter," Vols. I and II, AFFDL-TR-67-140, Aug. 1968, Air Force Flight Dynamics Lab.

[8] Shideler, J. L. et al., "Flutter at Mach 3 of Thermally Stressed Panels and Comparison with the Theory for Panels with Edge Rotationally Restrained," TN D-3498, Aug. 1966, NASA.

[9] Kordes, E. E. and Noll, R. B., "Theoretical Flutter Analysis of Flat Rectangular Panels in Uniform Coplanar Flow with Arbitrary Direction," TN D-1156, Jan. 1962, NASA.

[10] Olson, M. D., "On Applying Finite Elements to Panel Flutter," *AIAA Journal*, Vol. 5, No. 12, Dec. 1967, pp. 2267–2270.

[11] Olson, M. D., "Some Flutter Solutions Using Finite Elements," *AIAA Structural Dynamics and Aeroelasticity Specialists Conference*, AIAA, New York, 1969.

[12] Fralich, W. R., "Post Buckling Effects on the Flutter of Simply Supported Rectangular Panels at Supersonic Speeds," TN D-1615, March 1963, NASA.

NOVEMBER 1970 AIAA JOURNAL VOL. 8, NO. 11

Comparison of Theory and Experiment for Nonlinear Flutter of Loaded Plates

C. S. VENTRES* AND E. H. DOWELL†
Princeton University, Princeton, N. J.

The flutter behavior of clamped plates exposed to transverse pressure loadings, or buckled by uniform thermal expansion has been investigated theoretically, and the results compared with existing experimental data. Quasi-steady aerodynamic theory and von Kármán's plate equations are employed. Two sets of in-plane boundary conditions are considered: 1) zero in-plane motion normal to the edges, and 2) zero in-plane stress at the edges. A modal expansion of the transverse deflection is used in conjunction with Galerkin's method to obtain a set of nonlinear ordinary differential equations which are integrated numerically to determine the flutter motion. Good correlation is obtained between experimental and theoretical flutter boundaries for plates exposed to a static pressure differential. The stability boundaries of low aspect ratio plates with zero edge restraint are found to be more sensitive to pressure loads than are those of plates with complete edge restraint. Moreover, comparisons with available experimental data indicate that zero edge restraint is a good assumption for some panel configurations. Finally, it is indicated that fair agreement between theory and experiment can be obtained for buckled plates.

Nomenclature

a = plate length
a_n = modal amplitude
b = plate width
c = speed of sound
d = cavity depth
$D \equiv Eh^3/12(1-\nu^2)$ = plate stiffness
E = Young's modulus
h = plate thickness
I = area moment of inertia
$K \equiv \omega(\rho_m h a^4/D)^{1/2}$ = dimensionless radian frequency
k_x,k_y = in-plane spring constants
M = Mach number
N_x,N_y = in-plane stresses
p = pressure
$P \equiv pa^4/Dh$ = dimensionless pressure
t = time
u = plate in-plane displacement, x direction
U = flow velocity
v = plate in-plane displacement, y direction
w = transverse plate deflection
x,y,z = plate coordinates
α = coefficient of thermal expansion
α_x,α_y = in-plane restraint parameters [see Eq. (15)]
$\beta \equiv (M^2-1)^{1/2}$
Δp = static pressure differential
$\Delta P \equiv \Delta pa^4/D$ = dimensionless static pressure differential
ΔT = temperature differential
Δ_x,Δ_y = in-plane stretchings [see Eq. (5)]
$\mu \equiv \rho a/\rho_m h$ = dimensionless flow density
ν = Poisson's ratio
ρ = air density
ρ_m = plate density
$\tau \equiv t(D/\rho_m h a^4)^{1/2}$ = dimensionless time

Presented at the AIAA Structural Dynamics and Aeroelasticity Specialist Conference, New Orleans, La., April 16–17, 1969 (no paper number; published in bound volume of conference papers); submitted July 14, 1969; revision received March 13, 1970. This research was supported by NASA Grant 31-001-124.

* Research Associate.
† Associate Professor. Member AIAA.

Φ = Airy stress function
ω = radian frequency

Subscripts

f = flutter
p = peak
c = cavity

1. Introduction

THE general nature of the nonlinear (finite deflection) flutter behavior of flat plates has been discussed from a theoretical standpoint by several investigators,[1–3] none of whom treated the technically important case of a clamped-edge three-dimensional plate. As a result, detailed quantitative comparisons between the results they present and much of the experimental data published in the literature is impossible. In this paper, therefore, the nonlinear flutter of three-dimensional clamped plates is investigated theoretically. Primary emphasis is placed on making comparisons between theory and experiment.

The von Kármán plate equations are used to describe the elastic behavior of the plate. The nonlinear terms in these equations become important whenever deflections comparable to the plate thickness occur. Such deflections are known to occur during flutter. They also may occur prior to flutter if the plate is exposed to a static pressure differential between its upper and lower surfaces, or is buckled by in-plane compressive loads (which may be of either mechanical or thermal origin). In such situations the nonlinear theory is required not only to predict the amplitude and frequency of the limit cycle (flutter) motion, but also to predict the onset of the instability (the flutter boundaries). At present, very little quantitative experimental information is available on the amplitude of the flutter motion itself, but stability boundaries have been measured for pressure loaded and buckled plates.[4–7] Stability boundaries from Ref. 7 for pressure loaded plates and from Ref. 6 for buckled plates will be compared here with their theoretical counterparts to assess the accuracy of the nonlinear theory.

The aforementioned nonlinear terms in the von Kármán plate equations reflect the effect of structural coupling between the transverse plate deflection and in-plane membrane stresses induced by the deflection itself. However, the nature and distribution of these membrane stresses depend on the degree to which inplane motions of the plate edges are restrained. This restraint appears, in the structural theory used here, as the in-plane boundary conditions satisfied at the edges of the plate. Since these boundary conditions were not well defined in the experimental investigations chosen for the correlations, it has been found necessary to explore the extent to which inplane edge restraint conditions affect the flutter behavior of loaded plates. This has been done by deriving and solving plate equations of motion appropriate for the two limiting cases of complete and zero in-plane restraint, and by providing an approximate correction for the presence of partial restraint.

Some preliminary results of the investigation presented here have been reported in Ref. 8, and a more detailed account of the work is given in Ref. 9.

2. Problem Formulation

With a view toward making comparisons between theory and experiment, the panel geometry selected for consideration is shown in Fig. 1. The panel is a flat plate clamped at all four edges. The plate edges are, however, allowed to move in the plane of the plate, subject to elastic restraint. Beneath the plate is a sealed cavity, and over it, a uniform supersonic flow.

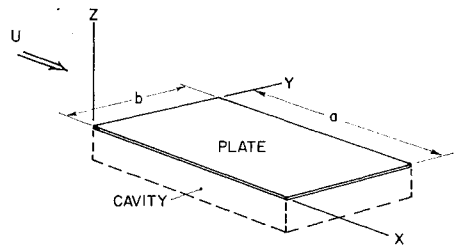

Fig. 1 Panel geometry.

Von Kármán's large deflection plate equations are used to describe the elastic behavior of the plate;

$$D\nabla^4 w + \rho_m h \frac{\partial^2 w}{\partial t^2} - \frac{\partial^2 \Phi}{\partial y^2}\frac{\partial^2 w}{\partial x^2} + 2\frac{\partial^2 \Phi}{\partial x \partial y}\frac{\partial^2 w}{\partial x \partial y} - \frac{\partial^2 \Phi}{\partial x^2}\frac{\partial^2 w}{\partial y^2} + p + \Delta p - p_c = 0 \quad (1)$$

$$\frac{1}{Eh}\nabla^4 \Phi = \left(\frac{\partial^2 w}{\partial x \partial y}\right)^2 - \frac{\partial^2 w}{\partial x^2}\frac{\partial^2 w}{\partial y^2} \quad (2)$$

In Eq. (1), p is the aerodynamic pressure loading due to the uniform supersonic flow. For high Mach numbers this pressure is given approximately by the usual quasi-steady expression

$$p = \frac{\rho U^2}{(M^2 - 1)^{1/2}}\left(\frac{\partial w}{\partial x} + \frac{1}{U}\frac{M - 2}{M - 1}\frac{\partial w}{\partial x}\right) \quad (3)$$

The other two pressure loading terms are, respectively, the static pressure differential Δp existing between the cavity and the external flow, and the acoustic pressure p_c created within the cavity by the plate motion. The static pressure differential is a given constant inhomogeneous term. For shallow cavities the acoustic pressure is approximated by the static expression

$$p_c = -\frac{\rho_c c^2}{abd}\int_0^a \int_0^b w dx dy \quad (4)$$

derived from the change in cavity volume due to the plate deflection.[10]

The influence of in-plane edge restraint is reflected in the in-plane boundary conditions satisfied at the plate edges. For most panel configurations the in-plane stresses and displacements on the boundary are functionally related, the nature of the relationship being dependent on the design of the particular panel support framework. Rather than attempting to represent exactly the inplane boundary conditions appropriate to any one panel configuration, in this paper two extreme cases will be considered. The first is that of a plate whose edges are completely restrained against in-plane motion. The boundary conditions appropriate for this situation are that $u = 0$ and $v = 0$ at the edges. However, for convenience in analysis these conditions will be modified to require that only the displacement normal to the edge vanish, and that the shear stress be zero. These latter boundary conditions have been shown to be a good "approximation" to the former set in the sense that modal expansions of the von Kármán equations satisfying each set exactly differ very little from each other.[11] The in-plane displacements u and v are related to the Airy Stress Function Φ through the stress displacement relations for the plate;

$$\frac{\partial u}{\partial x} + \frac{1}{2}\left(\frac{\partial w}{\partial x}\right)^2 = \frac{1}{Eh}\left(\frac{\partial^2 \Phi}{\partial y^2} - \nu\frac{\partial^2 \Phi}{\partial x^2}\right) + \alpha \Delta T$$

$$\frac{\partial u}{\partial y} + \frac{1}{2}\left(\frac{\partial w}{\partial y}\right)^2 = \frac{1}{Eh}\left(\frac{\partial^2 \Phi}{\partial x^2} - \nu\frac{\partial^2 \Phi}{\partial y^2}\right) + \alpha \Delta T$$

These can be integrated to compute the total stretchings $\Delta_x \equiv u(a,y) - u(0,y)$ and $\Delta_y \equiv v(x,b) - v(x,0)$:

$$\Delta_x = \frac{1}{Eh}\int_0^a \left(\frac{\partial^2\Phi}{\partial y^2} - \nu\frac{\partial^2\Phi}{\partial x^2}\right)dx - \frac{1}{2}\int_0^a \left(\frac{\partial w}{\partial x}\right)^2 dx + a\alpha\Delta T \tag{5}$$

$$\Delta_y = \frac{1}{Eh}\int_0^b \left(\frac{\partial^2\Phi}{\partial x^2} - \nu\frac{\partial^2\Phi}{\partial y^2}\right)dy - \frac{1}{2}\int_0^b \left(\frac{\partial w}{\partial y}\right)^2 dx + b\alpha\Delta T$$

Note that the thermal expansion due to a constant temperature rise ΔT has been included. Setting $\Delta_x = \Delta_y = 0$ is equivalent to requiring that the normal displacements vanish on the edges. Thus the boundary conditions are

$$\Delta_x = \Delta_y = 0 \text{ and } N_{xy} = 0 \text{ on the edges} \tag{6}$$

The second set of boundary conditions to be considered are those of a plate whose edges are completely unrestrained. The stresses then vanish at the plate edges. In terms of the Airy Stress Function Φ this requirement takes the form

$$\left.\begin{matrix}\Phi = 0\\ \dfrac{\partial\Phi}{\partial x} = 0\end{matrix}\right\} x = 0,a \qquad \left.\begin{matrix}\Phi = 0\\ \dfrac{\partial\Phi}{\partial y} = 0\end{matrix}\right\} y = 0,b \tag{7}$$

3. Method of Solution

3.1 Modal Expansion

The system of Eqs. (1–4) are transformed into a set of ordinary nonlinear differential equations by the Galerkin method, in which the deflection w is expanded in a series of modes that satisfy the appropriate boundary conditions. For a clamped plate the following expansion has been chosen:

$$w = \sum_{m=1}^{N} A_m(t)\psi_m\left(\frac{x}{a}\right)\psi_1\left(\frac{y}{b}\right) \tag{8}$$

$$\psi_m(x/a) \equiv \cos(m-1)(\pi x/a) - \cos(m+1)(\pi x/a) \tag{9}$$

Only one mode has been retained in the cross-stream direction. This approximation is motivated by the fact that the first cross-stream mode is known to be critical in the linear theory for the stability of flat, unbuckled plates. For buckled plates one cross-stream mode may not be sufficient; see Sec. 4.5 for further discussion on this point.

The series (8) is inserted into Eq. (2). This linear partial differential equation is solved for Φ, using boundary conditions (6) or (7). The manner in which this is done is described briefly below. Despite the choice of the simplest possible modal functions[9] appropriate for clamped plates, the calculations involved are extremely tedious, and the expressions arrived at very lengthy. Therefore, they will not be displayed completely here; only the general form of the equations will be given. Refer to Ref. 9 for details.

3.2 Complete In-Plane Edge Restraint

A particular solution Φ_p of Eq. (2) is easily found. This solution is outlined in Appendix 1. It will be written symbolically here as

$$\Phi_p = \sum_{m=1}^{N}\sum_{n=1}^{N} \Phi_{mn^p}(x,y)A_m(t)A_n(t) \tag{10}$$

If Φ_p and the series expansion (8) for w are inserted in relations (5), it is found that Δ_x and Δ_y are, respectively, independent of y and x. Therefore, a simple homogeneous solution to Eq. (2), corresponding physically to a uniform expansion of the plate, is added to Φ_p to form the complete solution

$$\Phi = \Phi_p + \tfrac{1}{2}(\bar{N}_x y^2 + \bar{N}_y x^2) \tag{11}$$

The total stretchings are now recalculated as

$$\Delta_x = a\alpha\Delta T + \frac{a}{Eh}(\bar{N}_x - \nu\bar{N}_y) - \sum_{m=1}^{N}\sum_{n=1}^{N}\Delta_{mn^x}A_mA_n$$

$$\Delta_y = b\alpha\Delta T + \frac{b}{Eh}(\bar{N}_y - \nu\bar{N}_x) - \sum_{m=1}^{N}\sum_{n=1}^{N}\Delta_{mn^y}A_mA_n$$

where

$$\Delta_{mn^x} \equiv \frac{1}{2a}\int_0^1 \psi_m'(\xi)\psi_n'(\xi)d\xi\cdot\psi_1^2\left(\frac{y}{b}\right) - \frac{1}{Eh}\int_0^a\left(\frac{\partial^2\Phi_{mn^p}}{\partial y^2} - \nu\frac{\partial^2\Phi_{mn^p}}{\partial x^2}\right)dx$$

and

$$\Delta_{mn^y} = \frac{1}{2b}\int_0^1 \psi_1^2(\xi)d\xi\cdot\psi_m'\left(\frac{x}{a}\right)\psi_n'\left(\frac{x}{a}\right) - \frac{1}{Eh}\int_0^b\left(\frac{\partial^2\Phi_{mn^p}}{\partial x^2} - \nu\frac{\partial^2\Phi_{mn^p}}{\partial y^2}\right)dy$$

To satisfy boundary conditions (6), Δ_x and Δ_y are set to zero, thus determining $\bar{N}_x$ and $\bar{N}_y$;

$$\bar{N}_x = -\frac{Eh\alpha\Delta T}{1-\nu} + \frac{Eh}{1-\nu^2}\times \sum_{m=1}^{N}\sum_{n=1}^{N}\left(\frac{\Delta_{mn^x}}{a} + \nu\frac{\Delta_{mn^y}}{b}\right)A_mA_n$$

$$\bar{N}_y = -\frac{Eh\alpha\Delta T}{1-\nu} + \frac{Eh}{1-\nu^2}\times \sum_{m=1}^{N}\sum_{n=1}^{N}\left(\frac{\Delta_{mn^y}}{b} + \nu\frac{\Delta_{mn^x}}{a}\right)A_mA_n$$

The solution Φ as given by Eq. (11) is found to satisfy $N_{xy} = 0$ on the plate edges without further modification. Note that the conditions $\Delta_x = 0$ and $\Delta_y = 0$ could not have been satisfied using the simple homogeneous solution $\frac{1}{2}(\bar{N}_x y^2 + \bar{N}_y x^2)$ had Δ_x and Δ_y not turned out to be independent of y and x.

3.3 Zero In-Plane Edge Restraint

The stress function Φ is expanded in a series of functions that satisfy boundary conditions (7);

$$\Phi = \sum_{m=1}^{N_x}\sum_{\substack{n=1\\(\text{odd})}}^{N_y}\Phi_{mn}(t)\psi_m\left(\frac{x}{a}\right)\psi_n\left(\frac{y}{b}\right) \tag{12}$$

where the ψ's are given in Eq. 9. The assumed form [Eq. (8)] for w is symmetric about the line $y = b/2$. The stress function Φ must share this symmetry, so that only the modes $\psi_n(y/b)$, $n = 1,3\ldots$ are included in the expansion (12). Galerkin's method is used to transform Eq. (2) into a set of simultaneous linear algebraic equations for Φ_{mn}

$$\sum_{m=1}^{N_x}\sum_{\substack{n=1\\(\text{odd})}}^{N_y}A_{klmn}\Phi_{mn} = \sum_{m=1}^{N}\sum_{n=1}^{N}G_{klmn}A_mA_n$$

$$k = 1,N_x;\quad l = 1,N_y \text{ (odd)}$$

The array A_{klmn} possesses a unique inverse A_{klmn}^{-1} that can be found numerically. The solution for Φ then has the form

$$\Phi = \sum_{m=1}^{N}\sum_{n=1}^{N}\left\{\sum_{p=1}^{N_x}\sum_{\substack{q=1\\(\text{odd})}}^{N_y}\sum_{r=1}^{N_x}\sum_{\substack{s=1\\(\text{odd})}}^{N_y}A_{pqrs}^{-1}\times G_{rsmn}\psi_p\left(\frac{x}{a}\right)\psi_a\left(\frac{y}{b}\right)\right\}A_mA_n$$

Normally, series expansions of the type (12) are only slowly convergent, since they must be differentiated twice to produce the in-plane stresses. However, in the present context the membrane stresses are not themselves of primary interest, but rather certain weighted integral averages of these stresses that appear in the modal equations to be discussed in Sec. 3.5. When N terms are retained in the modal expansion for w, it has been found that sufficient accuracy for the present purposes is realized by use of $N_x = 2N + 1$ and $N_y = 3$ in Eq. (12).

3.4 Finite Edge Restraint

The stress function (12) will now be modified to allow approximately for finite in-plane restraint. This is done by introducing averaged boundary conditions.[12] A simple homogeneous solution is added to the series (12):

$$\Phi = \sum_{m=1}^{N_x} \sum_{\substack{n=1 \\ (\text{odd})}}^{N_y} \Phi_{mn} \psi_m\left(\frac{x}{a}\right) \psi_n\left(\frac{y}{b}\right) + \frac{1}{2}(\bar{N}_x y^2 + \bar{N}_y x^2) \quad (13)$$

Since $\psi_m(x/a)$ and $\psi_n(y/b)$ satisfy boundary conditions (7), $\bar{N}_x$ and $\bar{N}_y$ are the in-plane stresses on the plate edges. These are made to be proportional to the average values of the total stretchings;

$$\begin{aligned} \bar{N}_x &= -k_x \frac{1}{b} \int_0^b \Delta_x dy \\ \bar{N}_y &= -k_y \frac{1}{a} \int_0 \Delta_y dx \end{aligned} \quad (14)$$

The result is

$$\bar{N}_x = -\frac{Eh\alpha_x}{1 - \nu^2\alpha_x\alpha_y}\left[(1 + \nu\alpha_y)\alpha\Delta T - \sum_{m=1}^{N}\sum_{n=1}^{N}(F_{mn} + \nu G_{mn})A_m A_n\right]$$

$$\bar{N}_y = -\frac{Eh\alpha_x}{1 - \nu^2\alpha_x\alpha_y}\left[(1 + \nu\alpha_x)\alpha\Delta T - \sum_{m=1}^{N}\sum_{n=1}^{N}(G_{mn} + \nu F_{mn})A_m A_n\right]$$

where

$$F_{mn} \equiv \frac{1}{2a^2}\int_0^1 \psi_m'(\xi)\psi_n'(\xi)d\xi \cdot \int_0^1 \psi_1^2(\xi)d\xi$$

$$G_{mn} \equiv \frac{1}{2b^2}\int_0^1 \psi_m(\xi)\psi_n(\xi)d\xi \cdot \int_0^1 \psi_1'^2(\xi)d\xi$$

$$\alpha_x \equiv ak_x/Eh + ak_x,\ \alpha_y \equiv bk_y/Eh + bk_y \quad (15)$$

It should be noted that boundary conditions (14) do not become equivalent to boundary conditions (6) when $k_x, k_y \to \infty$, because Eq. (14) then requires only that the *average* total stretching be zero.

3.5 Modal Equations of Motion

To complete the Galerkin procedure, the stress functions (11) or (13) are substituted along with the modal expansion (8) for w into Eq. (1). The resulting expression is multiplied successively by $\psi_i(x/a) \cdot \psi_i(y/b)$ and integrated over the area of the plate. A set of nonlinear ordinary differential equations in time is obtained. This set of equations has the following general form, in dimensionless notation:

$$\sum_{j=1}^{N} S_{ij}\frac{d^2a_j}{d\tau^2} = -\sum_{j=1}^{N}(C_{ij} + D_{ij})a_j - \left(\frac{M^2 - 2}{M^2 - 1}\right)\left(\frac{\mu\lambda}{\beta}\right)^{1/2}\sum_{j=1}^{N} S_{ij}\frac{da_j}{d\tau} - \sum_{j=1}^{N}\sum_{k=1}^{N}\sum_{l=1}^{N} B_{ijkl}a_j a_k a_l - \lambda_c\frac{a}{d}\delta_{1i}a_1 + \Delta P\delta_{1i} \quad (16)$$

In these equations the $a_i \equiv Ai/h$ are the (dimensionless) modal amplitudes, while λ, μ, ΔP, M, and $\lambda_c a/d$ are the flow dynamic pressure, flow density, static pressure differential, Mach number, and cavity density. Henceforth, the expression $[(M^2 - 2)/(M^2 - 1)](\mu\lambda/\beta)^{1/2}$ will be replaced by its asymptotic value for large Mach numbers, $(\mu\lambda/M)^{1/2}$. The quantities μ and M then appear only as the ratio μ/M. See Sec. 4.1 in this regard.

The symmetric matrices S_{ij} and C_{ij} are inertial and elastic coupling matrices, respectively. Matrix C_{ij} contains $\alpha\Delta T$ as a parameter; for sufficiently large $\alpha\Delta T$, the elements of C_{ij} change sign (plate buckling). The presence of nonlinear structural coupling between out-of-place bending and in-plane stretching is reflected in the array B_{ijkl}. This array contains α_x and α_y as parameters, and the values of the terms in the array depend on whether expression (11) or (13) has been used for Φ.

Equations (16) are solved by numerical integration. The panel configuration to be studied is defined by the material constant ν (Poisson's ratio), the plate length/width ratio a/b, and the boundary flexibility parameters α_x and α_y. The aerodynamic forces on the panel and in-plane loading are determined by λ, μ/M, ΔP, $\lambda_c a/d$, and $\alpha\Delta T$. The result of the integration is a time history of the modal amplitudes $a_i(\tau)$, $i = 1, \ldots N$, that can be used to study both the stability of the panel and the nature of its postflutter motion.

4. Results and Discussion

4.1 Preliminary Results

The plate response tine histories obtained in the manner described here are qualitatively similar to those described in Ref. 4, in which the nonlinear flutter of simply supported plates is treated. Therefore, the reader should consult that reference for a more detailed discussion of the following points, mentioned only briefly here.

The response time history of a plate that is stable in the linear sense corresponds to a decaying transient; the panel motion dies out with time. If the plate is linearly unstable, the motion develops into a periodic limit cycle. The limit cycle motion is a simple harmonic oscillation for unbuckled plates. For $a/b \lesssim 2$, the plate deflection is a standing wave, with some phase shift appearing for larger values of a/b. The largest deflection usually occurs near $x/a = 0.75$. The amplitude and frequency of the limit cycle oscillation generally do not depend on the initial conditions used to start the integration. Of course, if $\Delta p = 0$, Eqs. (16) are homogeneous, so that the initial conditions must be nonzero if a nontrivial response is to be obtained.

The flow density parameter μ/M is found to have only a minor effect on the panel response, when limited to its range of practical interest ($0.01 \lesssim \mu/M \lesssim 0.1$). Therefore, no attempt has been made to accurately match μ/M in comparing theory and experiment. Usually the convenient value $\mu/M = 0.1$ was used, primarily to decrease the time required for the initial transient to decay.

Finally, it has been found, as in Ref. 4, that 4 to 6 modes must be used in the modal expansion for ω to obtain quantitative accuracy. Six modes have been used to compute the results presented here.

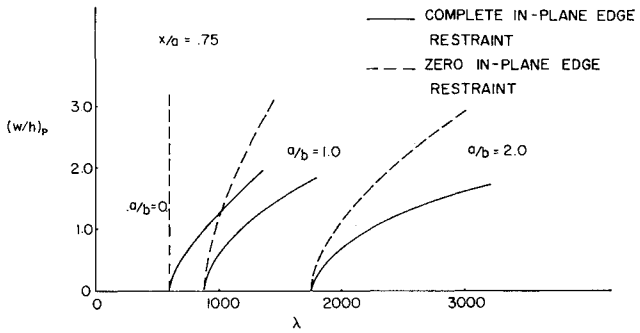

Fig. 2 Flutter amplitude vs dynamic pressure.

4.2 Unloaded Plates

In Figures 2 and 3 are shown the limit cycle amplitude and frequency for initially stress-free clamped plates, with and without in-plane edge restraint. Note in Fig. 2 that the presence or absence of in-plane restraint does not affect the flutter boundary (the value of λ for which $(w/h)_p \rightarrow 0$). This is to be expected, since the in-plane boundary conditions affect only the nonlinear terms in the equations of motion, and these have a negligible effect on small amplitude motions about the flat configuration. In-plane restraint conditions thus affect only the postflutter motion.

The amplitude of the limit cycle is greatest for plates without in-plane restraint. For two dimensional plates without in-plane restraint no final amplitude exists within the context of the present theory, since there are then no membrane stresses associated with the flutter motion. [This can be seen in Eq. (2). The right-hand side of this equation is proportional to the Gaussian curvature of the plate, which is zero for deflections independent of y. Any contribution to Φ must therefore come from the boundary conditions.] As a/b increases, however, the Gaussian curvature associated with the flutter motion increases, so that membrane stresses are created even in the absence of in-plane restraint at the edges. The ratio of the limit cycle amplitudes for plates with and without in-plane restraint therefore decreases as a/b increases (Fig. 2). The frequency of flutter is somewhat less for plates without in-plane restraint, as shown in Fig. 3, although the difference is small.

4.3 Natural Frequencies of Pressure Loaded Plates

A plate exposed to a transverse pressure load undergoes a static deformation that causes stretching in the middle surface of the plate. The membrane stresses associated with this stretching stiffen the plate, raising its natural frequencies of vibration. In-plane boundary support flexibility will relieve the membrane stresses and so change the natural frequencies of the loaded plate. Since it is known from the linear theory that the stability of a plate in a uniform airflow is governed by the relative spacing of its natural frequencies, it is important that the in-plane boundary conditions be known,

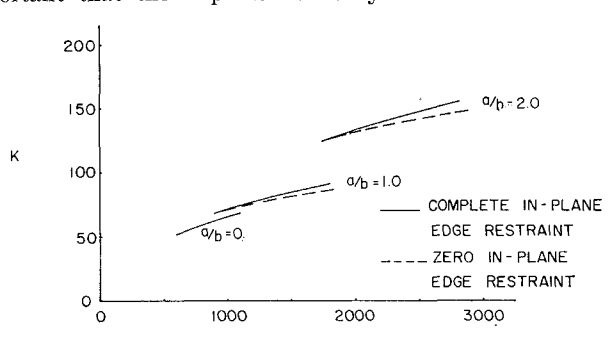

Fig. 3 Flutter frequency vs dynamic pressure.

and that their effect on the frequency spectra be understood. Moreover, the accuracy with which the natural frequencies can be computed provides an excellent test of the ability of Eqs. (16) to properly represent the elastic behavior of the plate.

Figure 4 shows the effect of a static pressure differential on the lowest three natural frequencies of a panel built and tested by the authors.‡ The panel consisted of an aluminum plate, 20 in. × 10 in. × 0.05 in., bonded onto a rectangular frame built up of aluminum rails welded together at the corners. Also shown in Fig. 4 are natural frequencies computed from the modal equations (16), for the limiting cases of zero and complete in-plane restraint. These calculations were carried out by setting $\lambda = 0$ in the equations of motion but using a nonzero value of $(\mu\lambda/M)^{1/2}$ to provide damping. The equations were integrated to find the static reflection under the pressure loading, and then linearized about this equilibrium configuration to determine the natural frequencies in the usual way.

Note that theory and experiment agree quite well at $\Delta p = 0$, but that the assumption of complete in-plane restraint considerably over estimates the frequencies for $\Delta p \neq 0$. The experimental data lie closest, in fact, to the curves for zero in-plane restraint. Presumably the rails to which the plate edges were bonded were sufficiently rigid to restrain them against rotation (thereby maintaining a "clamped" boundary condition), yet were unable to provide complete restraint against in-plane motions at the edges.

The plate natural frequencies have been recalculated in Fig. 5, using nonlinear terms B_{ijkl} computed from Eqs. (13). Values of α_x and α_y were estimated from measurements of the plate static deflection under the pressure load. (The static deflection data appeared in Ref. 8, and will not be repeated here.) The panel side rails were assumed to bend as simple beams under the in-plane loads caused by the plate deflection. The mean deflection of the side rails would then be proportional to the fourth power of their length, so that

$$k_x = C(EI/b^4),\ k_y = C(EI/a^4)$$

where EI is the common bending rigidity of the two sets of beams, and C is a dimensionless constant. These values of k_x and k_y were used to determine α_x and α_y from their definitions, Eqs. (15). It is also possible that some in-plane flexibility is provided by the relatively low shear modulus of the bond between the plate and frame. If this were the case, the appropriate ratio between α_x and α_y would be altered somewhat. However, calculations indicate that only the flexibility of the longer sides is important, so that this ratio is not critical. The value of C that provided the best match with the measured pressure static deflection data

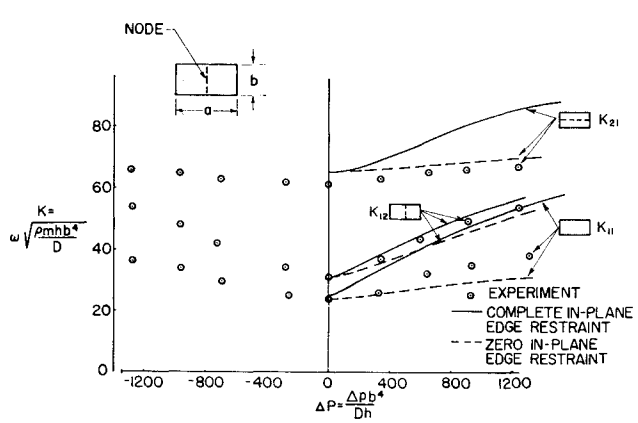

Fig. 4 Natural frequencies vs static pressure differential.

‡ Some of the results that follow were reported in Ref. 8.

was used to compute the plate natural frequencies shown in Fig. 5. The agreement between theory and experiment is now quite good for all values of Δp. Therefore, flutter calculations carried out with values α_x and α_y determined in the manner discussed previously should give improved agreement between theory and experiment.

4.4 Flutter of Pressure Loaded Plates

The results of the previous section indicate that in-plane restraint conditions play an important role in determining the natural frequencies of plates exposed to a static pressure differential. In this section flutter boundaries for pressure loaded plates with and without in-plane restraint will be determined, and compared with experimental results from Ref. 7. The results of vibration tests, taken from Ref. 7, and similar to those described in the previous section, will be used to obtain an independent estimate of the degree of edge restraint present in the panels used for the flutter experiments.

The panels tested in Ref. 7 consisted of aluminum alloy plates bonded onto a supporting framework with epoxy cement. The frames were built up of aluminum beams bolted and bonded together at the ends. For the two panels of interest here, the plates were 0.020 and 0.025 in. thick, and measured 8.5 in. × 18.5 in. between supports.§ These panels were designated as panels 10-20-20 and 20-10-25, respectively. For convenience, the same designations will be used here.

The natural frequencies of both panels were measured prior to the wind tunnel tests, while exposed to a static pressure loading. For this purpose a sealed cavity $2\frac{1}{2}$ in. deep was formed beneath the plate, and pressurized. Because of the small cavity depth, a pronounced cavity effect was present during the testing. The results of the vibration tests on panel 10-20-20 are shown in Fig. 6. Those for panel 20-10-25 are similar. Also shown are theoretical frequencies calculated in the same manner as described previously, with the exception that the effect of the cavity [in the form of the static cavity approximation, Eq. (4)], was included in the calculations.

Vibration tests of this sort are carried out by forcing air into the cavity until a preselected pressure is attained, and then measuring the natural frequencies of the panel. During the initial "pumping up" phase of the experiment the cavity is connected to a supply of compressed air, so that the cavity volume is effectively infinite. Therefore, in using the modal Eqs. (16) to calculate the static plate deflection caused by the pressure, the cavity parameter $\lambda_c(a/d)$ was set to zero. On the other hand, during the vibration tests the effective cavity volume is finite. The appropriate (nonzero) values of

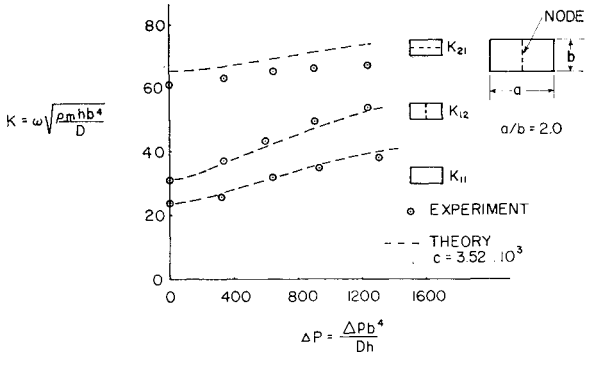

Fig. 5 Natural frequencies vs static pressure differential.

§ Not all the data for pressure loaded panels from Ref. 7 were used. However, the results presented here are typical, and inclusion of the remaining material would not change the conclusions reached.

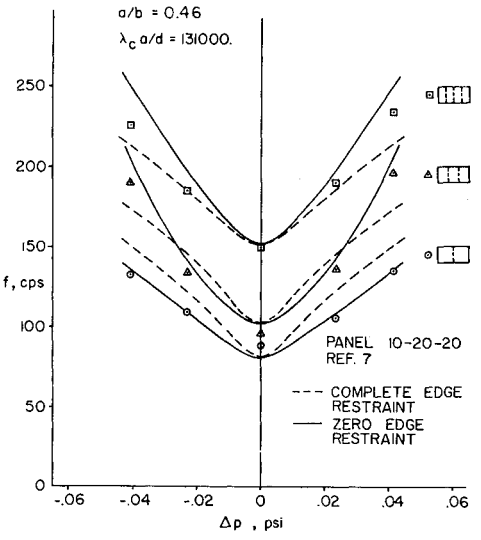

Fig. 6 Natural frequencies of pressure loaded plate.

$\lambda_c(a/d)$ were therefore included in the equations in computing the natural frequencies of the plate.

Figure 6 indicates clearly that an appreciable amount of in-plane flexibility was present. The experimental results lie closest to the curves calculated for zero restraint, as was the case for the panel mentioned in the previous section. This latter panel was similar in construction to the present ones.

It should be pointed out that a preliminary comparison of this same data with a nonlinear theory for two-dimensional plates gave no indication of the presence of in-plane support flexibility.[8] This misleading result was due to a failure to set the cavity parameter $\lambda_c(a/n)$ to zero in calculating the static equilibrium plate deflection, as discussed previously.

Panel 20-10-25 was mounted in the wind tunnel with its long sides parallel to the flow, so that in the present terminology, $a/b = 2.18$. Panel 10-20-20 was tested with its short side parallel to the flow, so that $a/b = 0.46$. The cavity was pressurized during the flutter testing. The panel stability boundaries were determined as a function of the pressure differential between the cavity and a static pressure tap located 1 in. upstream of the loading edge of the plates. The tunnel Mach number was 2.0 for all tests of interest here.

The stability boundaries obtained were not symmetric about $\Delta p = 0$. Since the flutter boundaries for a perfectly flat plate would have such symmetry, and since the measured natural frequencies shown in Fig. 6 give no indication that the two plates were not flat, the asymmetry is presumably due to streamwise pressure gradients in the mean tunnel flow, or to misalignment between the flow and the plate. Therefore, the data presented in Figs. 7 and 8 have been adjusted to make them symmetric about $\Delta p = 0$. This effectively assumes the existence of some equivalent constant Δp.

The theoretical flutter boundaries shown in Figs. 7 and 8 were obtained by computing the plate flutter amplitude for various values of ΔP at a fixed value of λ (or various λ at fixed ΔP, whichever proved most convenient), and then extrapolating to determine the point at which the flutter amplitude is zero. The effect of the cavity was included in the form of the static approximation, Eq. (4). In addition, experimentally determined values for the natural frequencies (for $\Delta p = 0$) of the two panels, taken from Ref. 7, were used to account approximately for the effects of imperfect panel construction. These frequencies characterize the linear elastic behavior of the panels. They were inserted in the modal equations (16) by selecting a change of variables $\dot{a}_i = \Sigma_i Q_{ij} a_j$ that simultaneously reduced the matrix S_{ij} to the identity matrix and C_{ij} to a diagonal matrix. The elements on the diagonal of C_{ij} were then the squares of the

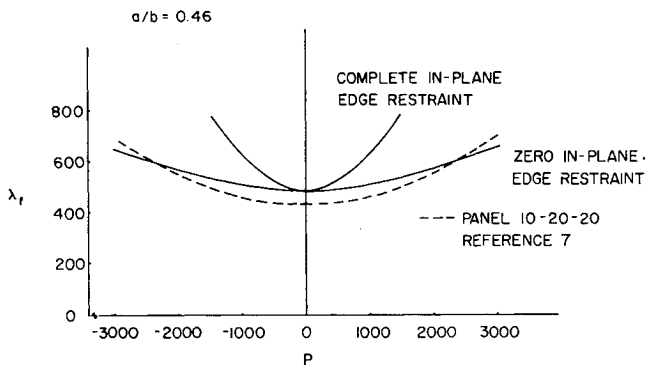

Fig. 7 Flutter dynamic pressure vs static pressure differential.

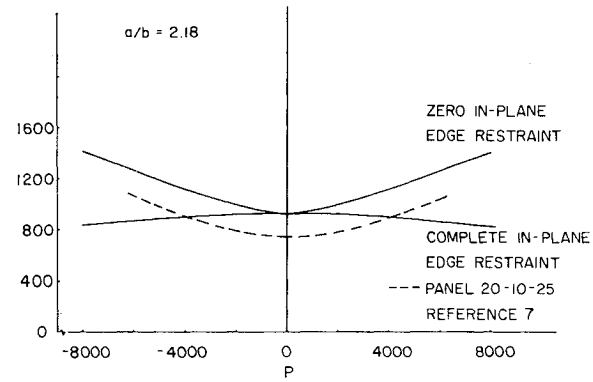

Fig. 8 Flutter dynamic pressure vs static pressure differential.

theoretical natural frequencies of the plate.[13] These were replaced by their measured counterparts, and the reverse transformation carried out. The other terms in Eqs. (16) were not affected by this process.

Note that the relative positions of the stability boundaries calculated for zero and for complete in-plane restraint are reversed in the two figures. Moreover, in Fig. 8 a pressure differential is seen to have a destablizing effect on the plate with complete restraint. These rather surprising results are consistent with the frequency spectra for the plate mentioned in Sec. 4.4 (Fig. 4). For $a/b = 2$, flutter is caused by aerodynamic coupling between the natural modes corresponding to K_{11} and K_{12}. The stability of the panel is dependent on the separation between these two frequencies. As seen in Fig. 4, the dependence of K_{12} on ΔP is not sensitive to the in-plane boundary conditions. On the other hand, K_{11} increases rapidly with ΔP for the case of complete in-plane restraint, but more slowly for zero restraint. The pressure differential, therefore, increases the separation between these two frequencies for zero restraint, but decreases the separation for complete restraint. The panel with zero restraint is thus stabilized by the pressure differential, while the one with complete restraint is somewhat destabilized, in agreement with Figs. 7 and 8.

It should be recognized that the behavior of a plate exposed to a pressure load depends not only on the membrane stresses caused by the load, but on the induced midplane curvature as well. For fully restrained plates, the effect of the tension is predominant, but for plates without in-plane restraint the influence of the curvature must be considered also. Previous investigators have sought to equate the effect of a static pressure differential solely to that of an equivalent in-plane tension.[14] This works fairly well for plates with complete in-plane restraint, but leads to the erroneous conclusion that unrestrained plates are not affected by pressure loads, for any a/b.[15] The results presented here show that this is so only for $a/b \ll 1$.

The best agreement between theory and experiment in Figs. 7 and 8 is obtained by assuming zero in-plane restraint. This is consistent with the correlation between the measured and calculated frequency spectra for the same two panels (Fig. 6), discussed earlier. From this it can be reasonably concluded that plates supported by seemingly massive support structures may behave as though relatively free of in-plane restraint, and that modal equations based on von Kármán's nonlinear plate equations provide reasonably accurate predictions of the flutter behavior of plates exposed to static pressure differentials.

4.5 Buckled Plates

The flutter behavior of buckled plates is more complicated than that of unbuckled plates, primarily because of the existence of more than one equilibrium configuration (more than one possible buckled shape). Under some conditions the plate indulges in a so-called "oil canning" behavior, in which it moves alternately from the neighborhood of one buckled configuration to another. The resulting flutter motion is not simple harmonic and may not even be periodic.[2] Moreover, the presence of more than one possible equilibrium configuration lends some credence to the existence of sustained flutter oscillations below the linear flutter boundary. Such motions have been computed numerically for buckled two-dimensional plates.[1]

Most experimental work has been done on plates buckled by thermal expansion.[4–6] Attempts to compare theory and experiment have been limited to the nonbuckled range by the absence of theoretical results for buckled three-dimensional plates with clamped edges. The effect of a static pressure differential, present during the flutter tests, was accounted for in a semiempirical manner.[4–6]

In this section the present nonlinear theory will be compared with experimental results from Ref. 6 for plates with a length/width ratio of 2.9, buckled by thermal expansion. The testing was done at Mach number 3 in a blow-down wind tunnel. The tunnel dynamic pressure was held constant during each run (or was varied in step-wise increments). The plate being tested was heated by the airflow so that the in-plane loading increased with time, exceeding the buckling value before termination of the run. With but few exceptions flutter occurred prior to buckling, and then ceased at some point subsequent to buckling, while the run was still in progress. The temperature of the plate at the inception of flutter (flutter start) and at the cessation of flutter (flutter stop) was recorded.

Temperatures were recorded at several points on the lower surface of the plate during each test. The temperature distribution was not constant, but the difference between the temperatures recorded near the edges differed by only 20% of the average temperature rise. Therefore, in what follows it will be assumed that the plates were heated uniformly by the flow, and consequently that the in-plane stresses were constant over the surface of the plate.

Unfortunately, the temperature of the framework on which the plate was mounted was not recorded, or at least not published. Therefore, it was not possible to determine unambiguously the temperature rise ΔT which best characterized the thermal stresses in the plate. However, the plates used were 0.081 in., 0.063 in., and 0.053 in. thick, whereas the frame on which they were mounted was about $\frac{3}{8}$ in. thick. It is, therefore, reasonable to surmise that the frame temperature did not change much during the short period (about 10–40 sec) of tunnel operation.

For a given temperature differential ΔT, the nature of the in-plane loading depends on the in-plane boundary conditions. If the edges are completely restrained against in-plane motion, the in-plane stresses N_x and N_y are equal, and $(a^2/D)N_x = (a^2/D)N_y = 12(1 + \nu)(a/h)^2\alpha\Delta T$. The

parameter $R_T \equiv 12(1 + \nu)(a/h)^2\alpha\Delta T$ will be used to describe the thermal loading on the plate, even though it may not be fully restrained. If the plate is not fully restrained, then the in-plane stresses are equal only if $\alpha_x = \alpha_y$:

$$\frac{a^2}{D} N_x = \frac{\alpha_x(1 + \nu\alpha_y)(1 - \nu)}{1 - \nu^2\alpha_x\alpha_y} R_T$$

$$\frac{a^2}{D} N_y = \frac{\alpha_y(1 + \nu\alpha_x)(1 - \nu)}{1 - \nu^2\alpha_x\alpha_y} R_T$$

The plates tested were riveted to their support frames. Apparently, no attempt was made to determine experimentally the effective boundary support flexibility of the resulting structure.

The assumption of complete in-plane edge restraint produces the flutter boundaries shown in Fig. 9. Flutter boundaries are shown for both $\Delta P = 0$ and $\Delta P = 5000$, which values bracket most of the measured pressure differentials reported in Ref. 6. Despite the spread in the experimental data, the agreement between theory and experiment in Fig. 9 is not good. Nevertheless, the theoretical stability boundaries do possess some qualitative resemblence to the experimental data. Both theory and experiment show a marked decrease in λ_f with increasing R_T, followed by an increase in the buckled regime. Moreover, the presence of a pressure differential is seen to eliminate the very low value of λ_f at the "elbow" in the flutter boundary for $\Delta P = 0$.

Since the elbow in the theoretical stability boundaries occured at or very near to the Euler buckling load $R_T \doteq 320$, and since it can be seen in the experimental data that no panel was observed to remain flat for $R_T > 1200$, it was decided to select values of α_x and α_y so that buckling would occur at $R_T = 1200$. This is equivalent to assuming that the airflow does not affect the static buckling load. In consideration of the riveted edge construction, the spring constants k_x and k_y in the boundary conditions (14) were assumed to be equal. The value of k_x and k_y that caused buckling to occur at $R_T = 1200$ was selected, and then α_x and α_y were computed from their defining relations (15). Using nonlinear terms B_{ijkl} based on Ref. 13, the stability boundaries shown in Fig. 10 were computed.

In Fig. 10, two flutter boundaries are shown in the buckled regime. The "linear" or "small disturbance" flutter boundary was computed using a buckled equilibrium configuration as an initial condition for the numerical integration of the modal equations of motion. On the other hand, calculations proceeding from a flat plate initial condition produced sustained flutter-like oscillations below this linear flutter boundary. Since the buckled shapes involved deflections on the order of several plate thicknesses, this is physically equivalent to applying a large disturbance to the plate. These oscillations may have been only extended transients, although the integrations was continued out to $\tau \doteq 11$. (On this same

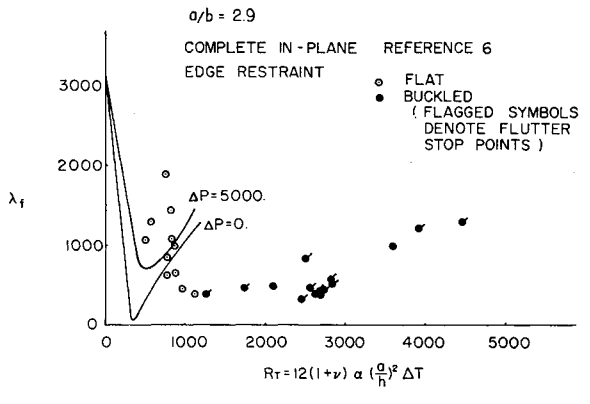

Fig. 9 Flutter dynamic pressure vs temperature differential.

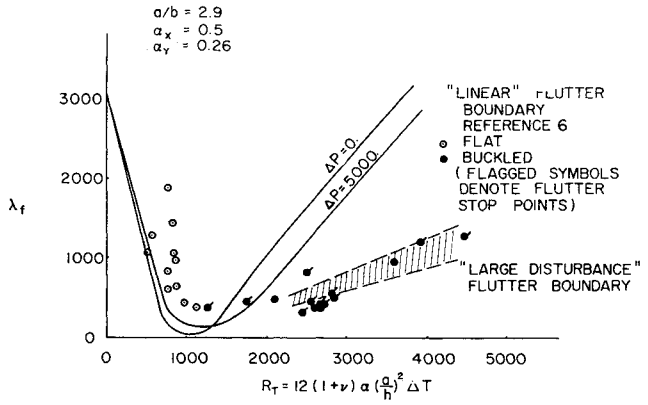

Fig. 10 Flutter dynamic pressure vs temperature differential.

time scale, the "frequency" of the motion was about 20, so that some 220 "cycles" were computed.) Nevertheless, the numerical results obtained do suggest that sustained flutter oscillations are possible for λ, R_T combinations above the shaded area in Fig. 10. Note that this "large disturbance" flutter boundary is in excellent agreement with the experimental data, since most of the data in that region are flutter stop points. The existence of two flutter start points in the same region is not explained by the large disturbance flutter boundary, however. It is also possible that some of the discrepancy between the experimental data and the linear flutter boundary can be explained by the existence of cross-steam coupling,[16] involving higher spanwise modes not included in the modal expansion (8) for w.

The flutter motion computed from the present theory agrees qualitatively with descriptions of the behavior observed experimentally. The plate motion is not simple harmonic, nor strictly periodic, but the peak deflections attained are repetitive. The motion is of the traveling wave variety, with two half wavelengths along the length of the plate. The buckled equilibrium shapes computed below the large disturbance flutter boundary consisted of two half wavelengths as well. Since the motion computed was not exactly periodic, an equivalent radian frequency was calculated by multiplying the number of amplitude peaks encountered per unit time (averaged over an extended time interval) by π. This frequency, shown in Fig. 11, is in generally good accord with the experimental data for all values of R_T. The band of frequencies shown were obtained for values of λ just above the large disturbance flutter boundary (for $R_T > 1200$), since these correspond to those observed in the experiments.

5. Conclusions

The flutter behavior of plates exposed to static transverse loads and in-plane loads has been studied theoretically, and

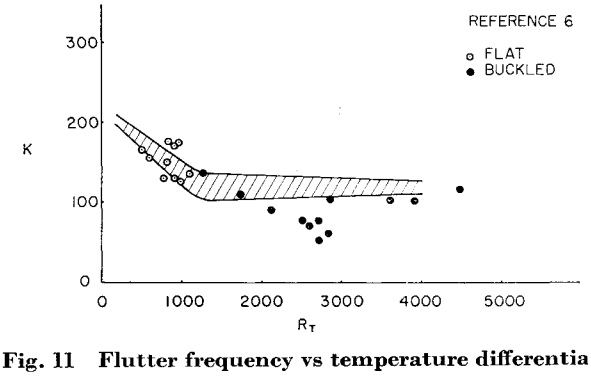

Fig. 11 Flutter frequency vs temperature differential.

the results compared with available experiment data. Von Kármán's nonlinear plate equations were used to formulate modal equations for the motion of a clamped plate in a uniform supersonic stream. Quasi-steady (high Mach number) aerodynamic theory was used.

The inplane boundary conditions satisfied at the edges of the plate were found to have an important effect on the behavior of the plate whenever it is forced to undergo large deflections. Therefore, the natural frequencies of a panel exposed to a transverse pressure load were measured experimentally to gain some indication of the degree of in-plane restraint that might be expected in practice. The panel tested was similar in construction to the type commonly used in wind-tunnel flutter tests. Comparison of the measured frequencies with values calculated for plates with complete and with zero inplane restraint, indicated that the panel behavior was more closely represented by the assumption of zero restraint than complete restraint. The degree of edge restraint actually present was estimated by matching calculated and measured values for the plate static deflection under pressure. Use of this estimated support flexibility in the natural frequency calculations provided excellent agreement between the calculated and measured natural frequencies of the plate.

Calculations made for the flutter boundaries of plates exposed to a static pressure differential also demonstrated the importance of in-plane edge restraint. It was found that edge support flexibility decreases the stabilizing effect of the static pressure differential for high aspect ratio plates, but increases it for low aspect ratio plates. In particular, and contrary to previously published statements,[15] low aspect ratio plates without edge restraint are strongly influenced by static pressure differentials. Comparison of the calculated stability boundaries with available experimental results show good correlation, but demonstrate the importance of determining the appropriate inplane support conditions in all future flutter test work. It is suggested that panel static deflection and/or natural frequency measurements of the type described in Sec. 4.3 be used for this purpose.

For plates exposed to static pressure loads and buckled by uniform thermal expansion, the present theory gives fair agreement with experiment. Numerical evidence is presented for the existence of sustained flutter motions below the linear stability boundary, for a clamped plate with $a/b = 2.9$. For thermally buckled plates the in-plane boundary conditions influence both the buckling temperature and the large-deflection elastic behavior of the plate. Proper definition of these boundary conditions during future experiments would make possible more precise comparisons with the nonlinear theory presented here. A simple thermal buckling experiment, in which the plate is heated radiantly in its mounting frame until it buckles, would be a good first step.¶ The mean plate temperature at buckling and the mode of buckling could be used to estimate the gross boundary support flexibility, and the relative flexibilities of the long and short sides of the plate.

Appendix

When expression (8) is inserted into Eq. (2), the right-hand side of Eq. (2) can be expressed as a sum of products of trigonometric functions of x/a and y/b. The particular solution is obtained by assuming a solution of the same form, containing an arbitrary multiplicative constant. This constant is evaluated by substituting the assumed solution into Eq. (2) and equating like terms on each side of the equation. The resulting solution has the form given in Eq. (10), in which $\Phi_{mn}{}^{p}(x,y)$ is an elaborate combination of trigonometric functions of x/a and y/b.

¶ The vibrational behavior of buckled plates is discussed in Ref. 17.

References

[1] Fung, Y. C., "On Two-Dimensional Panel Flutter," *Journal of the Aeronautical Sciences*, Vol. 25, No. 3, March 1958, pp. 145–160.

[2] Dowell, E. H., "Nonlinear Oscillations of a Fluttering Plate," *AIAA Journal*, Vol. 4, No. 7, July 1966, pp. 1267–1275.

[3] Fralich, R. W., "Post Buckling Effects on the Flutter of Simply-Supported Rectangular Panels at Supersonic Speeds," TN D-1615, 1963, NASA.

[4] Dixon, S. C., "Experimental Investigation at Mach Number 3.0 of Effects of Thermal Stress and Buckling on Flutter Characteristics of Flat Single-Bay Panels of Length-Width Ratio 0.96," TN D-1485, 1962, NASA.

[5] Dixon, S. C. and Shore, C. P., "Effects of Differential Pressure, Thermal Stress and Buckling on Flutter of Flat Panels with Length-Width Ratio of 2," TN D-1949, 1963, NASA.

[6] Shideler, S. L., Dixon, S. C., and Shore, C. P., "Flutter at Mach 3 of Thermally Stressed Panels and Comparisons with Theory for Panels with Edge Rotational Restraint," TN D-3498, 1966, NASA.

[7] Dowell, E. H. and Voss, H. M., "Experimental and Theoretical Panel Flutter Studies in the Mach Number Range 1.0 to 5.0," ASD-TDR-63-449, June 1963, Aeronautical Systems Division; also *AIAA Journal*, Vol. 3, No. 12, Dec. 1965, pp. 2292–2304.

[8] Dowell, E. H. and Ventres, C. S., "Nonlinear Flutter of Loaded Plates," *AIAA/ASME 9th Structures, Structural Dynamics and Materials Conference*, AIAA, New York, 1968.

[9] Ventres, C. S., "Nonlinear Flutter of Clamped Plates," Ph.D. thesis, Nov. 1969, Dept. of Aerospace and Mechanical Sciences, Princeton Univ., Princeton, N. J.

[10] Dowell, E. H. and Voss, H. M., "The Effect of a Cavity on Panel Vibration," *AIAA Journal*, Vol. 1, No. 2, Feb. 1963, pp. 476–477.

[11] Dowell, E. H. and Ventres, C. S., "Modal Equations for the Nonlinear Flexural Vibrations of a Cylindrical Shell," *International Journal of Solids and Structures*, Vol. 4, No. 10, Oct. 1968, pp. 975–991.

[12] Bolotin, V. V., *Nonconservative Problems in the Theory of Elasticity*, Macmillan, New York, 1963, pp. 274–312.

[13] Hildebrand, F. B., *Methods of Applied Mathematics*, 2nd ed., Prentice Hall, Englewood Cliffs, N. J., 1965, pp. 69–72.

[14] Lemley, C. E., "Design Criteria for the Prediction and Prevention of Panel Flutter," Vol. 2, AFFDL-TR-67-140, 1968, Air Force Flight Dynamics Lab.

[15] Lemley, C. E., "Design Criteria for the Prediction and Prevention of Panel Flutter," Vol. 1, AFFDL-TR-67-140, 1968, Air Force Flight Dynamics Lab.

[16] Fralich, R. W. and McElman, J. A., "Flutter of Buckled Simply-Supported Rectangular Panels at Supersonic Speeds," TN D-4357, 1968, NASA.

[17] Bisplinghoff, R. L. and Pian, T. H. H. "On the Vibration of Thermally Buckled Bars and Plates," *Proceedings of the Ninth International Congress of Applied Mechanics*, Brussels, 1956.